Novel Trifluoromethylated Enobosarm Analogues with Potent Anti-androgenic Activity *in vitro* and Tissue Selectivity *in vivo.*

D. Alwyn Dart [a,c] , Sahar Kandil [b] , Serena Tommasini-Ghelfi [c], Gilberto Serrano de Almeida [c], Charlotte L. Bevan [c], Wenguo Jiang [a], and Andrew D. Westwell [b]

[a] Cardiff China Medical Research Collaborative, Cardiff University School of Medicine, Cardiff, CF14 4XN, Wales, UK. [b] School of Pharmacy and Pharmaceutical Sciences, Cardiff University, Redwood Building, King Edward VII Avenue, CF10 3NB Cardiff, Wales, UK. [c] Androgen Signalling Laboratory, Department of Surgery & Cancer, Imperial College London, Hammersmith Hospital Campus, London, W12 0NN, UK.

These authors contributed equally to this manuscript

Running title: Potent anti-androgenic enobosarm analogues for prostate cancer treatment.

Corresponding author: dartd@cardiff.ac.uk

Keywords: prostate, cancer, enobosarm, anti-androgen, therapeutics

Conflict of Interest

The authors declare that there are no conflicts of interest in relation to the work described.

Abstract

Prostate cancer often develops anti-androgen resistance, possibly via androgen receptor (AR) mutations which change antagonists to agonists. Novel therapies with increased anticancer activity, whilst overcoming current drug resistance are urgently needed. Enobosarm has anabolic effects on muscle and bone whilst having no effect on the prostate. Here we describe the activity of novel chemically modified enobosarm analogues. The rational addition of *bis*-trifluoromethyl groups into ring B of enobosarm, profoundly modified their activity, pharmacokinetic and tissue distribution profiles. These chemical structural modifications resulted in an improved AR binding affinity - by increasing the molecular occupational volume near helix 12 of AR. *In vitro*, the analogues **SK33** and **SK51** showed very potent antiandrogenic activity, monitored using LNCaP/AR-Luciferase cells where growth, PSA and luciferase activity were used as AR activity measurements. These compounds were 10-fold more potent than bicalutamide and 100-fold more potent than enobosarm within the LNCaP model. These compounds were also active in LNCaP/BicR cells with acquired bicalutamide resistance. *In vivo*, using the AR-Luc reporter mice, these drugs showed potent AR inhibitory activity in the prostate and other AR-expressing tissues e.g. testes, seminal vesicles and brain. These compounds do not inhibit AR activity in the skeletal muscle, and spleen - thus indicating a selective tissue inhibitory profile. These compounds were also active *in vivo* in the *Pb-PTen* deletion model. **SK33** and **SK51** have significantly different and enhanced activity profiles compared to enobosarm, and are ideal candidates for further development for prostate cancer therapy with potentially fewer side effects.

Introduction

Prostate cancer (PCa) is the most commonly diagnosed male cancer in the Western world (1). Tumor growth is initially androgen dependent - driven by the androgen receptor (AR). Androgen receptor (AR) signalling pathway remains a key driver of PCa, implicated throughout the different stages of the disease, and as such represents an obvious therapeutic target in PCa therapy (2, 3). Androgen receptor (AR) is a member of the family of steroid hormone receptors, which are ligand-dependent transcriptional regulators for diverse sets of genes involved in both reproductive and anabolic actions (4-6). The prototypical model for AR involves ligand binding that induces conformational changes in the ligand-binding domain (LBD), revealing a co-activator dimerization surface composed of helices 3, 5, and 12, as the LBD site is adjacent to helix 12 (H12).

Currently, the mainstays of prostate cancer treatment are androgen ablation (to castrate levels) and/or antiandrogen treatment, which block AR signalling (2, 3). The major anti-androgens in clinical use are bicalutamide and enzalutamide (and historically flutamide, hydroxyflutamide and nilutamide) (Figure 1A). However, these compounds bind to AR with low affinity and can induce escape mechanisms. Furthermore, under AR amplification or mutation conditions some of these compounds exhibit agonist activity and fail to inhibit AR. This resistance may arise from, among other mechanisms, mutations to several key residues in the ligand-binding domain (AR-LBD) (7, 8). Common mutations in AR found in PCa patients include T877A, W741L, and W741C. Bicalutamide (Figure 1A) can act as an agonist in AR^{W741L} and AR^{W741C} while hydroxyflutamide is an agonist in AR^{T877A} (7, 8). Gain of function mutations are common in prostate cancers and are correlated with disease progression, the lack of therapeutic response and poor clinical outcomes. Additionally, AR mutations may be selected for during anti-androgen therapy – reviewed in (9, 10) .

Additionally, the use of anti-androgens in patients may elicit moderate side effects e.g. muscle wastage, bone density loss and CNS dysfunction – which are exacerbated in elderly men. Therefore, there is a growing need for selective androgen receptor modulators (SARM) that would demonstrate tissue-selective activity – being inhibitors of the AR in the prostate with tissue sparing effects elsewhere (11).

Enobosarm (also referred to as Ostarine™, GTx-024 or S-22) is a non-steroidal selective androgen receptor modulator (SARM) with a favourable safety and pharmacokinetic profile (Figure 1B). It belongs to the class of arylpropionamides, which are structurally derived from the antiandrogen bicalutamide. Enobosarm binds to and activates the AR with enantioselective affinity, potency and efficacy similar to, but somewhat less than, that of DHT (12). Transient transfection studies indicate that enobosarm is remarkably selective for the AR and it does not cross-react with other nuclear hormone receptors. This receptor specificity differentiates enobosarm's pharmacology from other

steroidal androgens and has likely contributed to observations that the drug has generally been well tolerated in clinical trials. It has selective anabolic effects and is under clinical development for prevention and treatment of muscle wasting (cachexia) in cancer patients (13, 14).

Results

Rational design of novel Enobosarm analogues

Nonsteroidal anti-androgens such as bicalutamide act as AR antagonists (Figure 1A), thus preventing androgen-dependent cell growth. In contrast, AR agonists e.g. enobosarm (Figure 1B) may act as agonists in all the AR LBD mutants, since they will fit sterically better with the bulk-reducing AR mutations than in AR^{wt} (15). The difference in activity between agonists such as enobosarm and antagonists such as bicalutamide in AR^{wt} may arise from the linker oxygen's smaller size relative to the sulfonyl group of bicalutamide (Figure 1A&B). This bulk in AR antagonist structure, though small, is thought to push the AR helix 12 away from the binding pocket, disturbing the agonist conformation of the androgen receptor (16). The current theoretical key to antagonism states that the differences observed among AR modulators (agonist or antagonist) are not because of their B-ring size or shape but because of their linker size and orientation (17). The improved understanding is being applied to rationally designed treatment options with novel mechanisms of action. It is proposed that AR antagonists should have appending molecular extensions to the core structure of AR agonists that interfere with the placement of H12, thereby disrupting co-activator recruitment (16, 18, 19).

In the enobosarm/AR^{wt} co-crystal structure (PDB code; 3RLJ)(17) (Figure 2A&B)**,** the 4-cyanophenyl ether group of enobosarm is situated between residues of H12 and the indolyl side chain of Trp^{741}, suggesting that in the wild-type receptor (and probably the W741L mutant) the larger substitution with the same orientation of the linker would result in a better AR antagonist by pushing against Helix 12. We tested this hypothesis in silico by investigating whether the introduction of 3,5-*Bis*-trifluoromethyl (3,5-*Bis*-CF_3) into B ring of enobosarm would provide the geometric bulk needed to keep ring B towards Helix 12 of AR. Preliminary molecular modelling studies showed that the *bis*-trifluoromethyl phenyl moiety (ring B in **SK33** and **SK51**) has significantly changed the orientation of ring B so that the (3,5-*Bis*-CF_3) groups are pointing outwards away from Trp^{741} and towards helix 12, thus preventing AR from adapting the AR agonist conformation, whilst keeping the small size of the oxygen linker. The combination of the small oxygen linker and the steric hindrance of the (3,5-*Bis*-CF_3) substitution on ring B resulted in the optimum size and orientation of ring B to impose conformational restriction away from Trp^{741} and towards helix 12 (Figure 2C & D). A small library of AR antagonists having the (3,5-Bis-CF_3) motif was prepared (20) among which **SK33** showed the best antiproliferative and metabolic profiles, hence it was selected for further studies.

The introduction of fluorinated substituents into drug candidates can impart a unique set of properties owing to the unique combination of electronegativity, size and lipophilicity features of fluorinated groups (21-25). These factors can have a substantial impact on the molecular

conformation, which in turn affect the binding affinity to the target protein (26, 27).

Chemical synthesis of SK33 and SK51

Racemic enobosarm derivatives (**SK33** and **SK51**) were prepared by reacting methacryloyl chloride (**2**) with the corresponding substituted anilines **1a** and **1b** in dimethylacetamide (DMA) solvent to obtain phenylacrylamides **3a** and **4b** which were converted into the corresponding epoxides **4a** and **4b** in the presence of a large excess of hydrogen peroxide and trifluoroacetic anhydride in dichloromethane (DCM). Opening of the epoxide rings of **4a** and **4b** with substituted 3,5-*bis* (trifluoromethyl)phenol (**5**) in tetrahydrofuran (THF) gave the final compounds **SK33** and **SK51**. The structures of the synthesised compounds were confirmed using analytical and spectroscopic data (^{1}H NMR, ^{13}C NMR, ^{19}F NMR and mass spectrometry), which were in full accordance with their depicted structures. **SK33** and **SK51** were purified (>95% as confirmed by HPLC) and tested as racemic mixture (Figure 1C).

Cellular activity of enobosarm and the trifluoromethylated analogues SK33 and SK51

The antiproliferative and selective activities of these compounds were tested *in vitro* in a panel of prostate cancer cell lines, namely LNCaP, VCaP, PC3 and Du145. LNCaP and VCaP represent prostate cells which have retained the expression of the androgen receptor (28, 29). However, LNCaP cells overexpress a mutant AR, with a T877A mutation in the ligand binding site. The VCaP cell line overexpresses wild type AR. Both cell lines are responsive to androgens and cells will express androgen responsive genes. The PC3 and Du145 cells do not express the AR nor do they express androgen responsive genes.

Cells were exposed to increasing concentrations of anti-androgens for 96 hours and cell viability was analysed using the MTT assay. In LNCaP^{AR+ve} cells the parental compound enobosarm, showed insignificant activity with the IC_{50} = 40 μM, however, the trifluoromethylated enobosarm analogue, **SK33**, demonstrated a significantly potent activity with IC_{50} = 0.2 μM (Figure 3A). Moreover, when compared to the antiandrogen bicalutamide, the novel compounds showed an increased efficacy (Figure 3B). **SK51** also displayed an increased activity compared to bicalutamide (IC_{50} = 0.7μM) (Figure 3B).

In PC3^{AR-ve} cells, enobosarm showed activity only at relatively high dose (Figure 3C), whilst **SK33** showed some moderate activity. When compared to bicalutamide, **SK33** showed a significantly increased increased activity. On the other hand, the anti-proliferative activity of

SK33 in LNCaP^{AR+ve} cells was over ten times higher than that of its activity against PC3^{AR-ve} cell line (Figure 3D).

Furthermore, the panel of prostate cancer cell lines were screened for their expression of the target androgen receptor (AR) by qPCR. As expected, LNCaP^{AR+ve} and VCaP^{AR+ve} cells showed robust expression of AR whilst AR was not detectable in PC3^{AR-ve} and Du145^{AR-ve} cells (Figure 3E).

Figure 3F depicts the summary of the activity profile of the **SK33** and **SK51** compounds in the four PCa cell lines where a clear activity difference (selectivity) can be observed between the AR^{+ve} cell lines (LNCaP and VCaP) and the AR^{-ve} cell lines (PC3 and Du145).

SK33 decreases cells entering S-phase in LNCaP cells but not in PC3 cells

To further analyse the activity of these compounds in prostate cancer cell lines we treated LNCaP (AR^{+ve}) or PC3 (AR^{-ve}) cells with 10μM of antiandrogen (or vehicle DMSO) for 48 hours. These cell lines were collected for FACS analysis and standard cell cycle profiling using propidium iodide staining for DNA content, was carried out.

LNCaP cells showed a decrease in the number of cells in S phase with all the anti-androgen compounds. **SK33** showed the highest reduction of the number of cells in S phase, followed by **SK51**, enzalutamide and then bicalutamide, respectively. (Figure 3G). No apparent cell toxicity could be visualised as estimated by the absence of a sub-G1 population or fragmented necrotic cells (Figure 3G). In the PC3 cell line, no significant effect was observed with any of the tested compound (Figure 3H). However, a small increase in G2/M phase could be detected with **SK33** in PC3 cells.

SK33 reduces AR transcriptional activity

We then analysed the ability of **SK33** to inhibit the activity of the AR protein *i.e.* the ligand activated transcription factor activity. The LNCaP/Luc cell line, has an integrated luciferase reporter gene under the specific control of the AR transcription factor, as shown in the schematic figure 4A (30). Growing these LNCaP/Luc cells in charcoal stripped serum for 72hours removes exogenous androgens and reduced the expression of AR-responsive genes down to a baseline level, as monitored by qPCR. Adding a synthetic androgen (R1881) back into the media (0-10nM) increased both PSA and Luciferase gene expression in a dose dependent manner (Figure 4B). Androgen treatment does not affect G418 gene expression

(coexpressed from the same integrated plasmid as the luciferase reporter) nor did it affect the expression of housekeeping genes L19, β-actin and GAPDH. The ability of the anti-androgens to block this androgen-dependent gene upregulation was then further tested. Treating hormonally starved LNCaP cells with R1881 showed a 9-fold upregulation of the endogenous gene PSA. When treated with increasing doses of either bicalutamide or SK33 a dose dependent inhibition of gene expression was seen. SK33 showed a greater PSA inhibition than bicalutamide at 1 and 10μM (Figure 4C). Conversely, the parental compound, enobosarm, showed a mild stimulatory activity (Figure 4D).

We then examined the real-time activity of AR in live LNCaP/Luc cells in response to increasing doses of **SK33** compared to the parental compound enobosarm and the anti-androgen bicalutamide. Live imaging and photon flux measurements of LNCaP/Luc cells grown on 96 well plates in the presence of 0-100μM compound for 24 hours resulted in a strong inhibition of AR-mediated luciferase activity (Figure 4E). The AR inhibitory concentration [50%] for both **SK33** and bicalutamide were approx. 1μM. Bicalutamide showed no further inhibitory effects past this concentration. However, **SK33** maintained a dose dependent inhibition, completely inhibiting the AR-mediated luciferase activity at 50-100μM concentration (Figure 4F).

SK33 and SK51 are active in LNCaP cells with acquired bicalutamide resistance.

LNCaP cells were grown in increasing concentrations of bicalutamide for 3-6 months, until proliferation was seen. This bicalutamide resistant cell line (LNCaP/BicR) then grew well in 20μM bicalutamide, with cell cycle kinetics similar to that of the parental cell line. An increased expression level of AR was seen in this cell line upon qPCR analysis (Figure 5A). Treating this cell line with increasing doses of bicalutamide showed a proliferative response – at 20-25μM, whereas the parental cell line showed sensitivity and an IC_{50} of 3μM (Figure 5B). The LNCaP/BicR cell line also showed a partial cross-resistance to enzalutamide (IC_{50} = 5μM approx.), Figure 5C. We then analysed if the mechanism of the acquired resistance to bicalutamide extended to the novel agents **SK33** and **SK51**. Treatment of LNCaP/BicR cells with increasing concentrations of **SK33** and **SK51** for 96hours resulted in a dose-dependent response and an inhibition of cell growth, rather than being proliferative agents as bicalutamide (Figure 5D), with IC_{50} of approximately 2μM for **SK51** and 5μM for **SK33**.

Although not as active as in the parental sensitive cell line, **SK51** did show an improved activity over enzalutamide (& bicalutamide).

In vitro aqueous solubility and microsomal metabolic stability

Subsequently, an early *in vitro* pharmacokinetic study of the most promising compound, **SK33**, was performed. The metabolic stability of SK33 was tested in human liver microsomes, where compounds were incubated for 45 min with pooled liver microsomes and the intrinsic clearance (CL_{int}) and half-life ($t_{1/2}$) values were calculated based on 5 time points. Compound **SK33** is characterised by an increased metabolic stability in comparison with the standard – bicalutamide (see Table 1). **SK33** has microsomal half-life ($t_{1/2}$) of 32 hr, which compares to that of standard drugs (bicalutamide and enzalutamide) and represents a good starting point for optimisation towards a weekly or twice-weekly administrable product. No observed *in vitro* cardiotoxicity was observed in our preliminary studies (7.6 % inhibition of hERG at 25μM concentration) (http://cyprotex.com). Because of these promising *in vitro* properties and the potent anti-proliferative profile in prostate-cancer cell lines, **SK33** was selected for more detailed pre-clinical *in vitro* and *in vivo* studies.

SK33 is a potent inhibitor of AR in the ARE-Luc reporter mouse – and shows tissue specificity

The transgenic ARE-Luc mouse model shows AR-driven luciferase activity in all tissues in response to androgen action and activity can be monitored in live animals in real time (31). Using age-matched male mice (littermates) we analysed the basal AR-driven luciferase levels in mice prior to treatment. ARE-Luc mice were injected with *D*-luciferin and imaged using an IVIS CCD camera in order to obtain baseline visualisation and measurements of androgen receptor tissue activity. ARE-Luc mice were then injected sub-cutaneously with 50mg/kg bicalutamide, **SK33** or vehicle (DMSO) control and left for 24 hours (n=3 for each treatment), after which the mice were imaged again under the exact same conditions. Post treatment mice were imaged again for luciferase activity (Figure 6A). Luciferase activity was measured from three regions of interest (ROI), including the head, abdominal and gonadal region (Figure 6B). Bicalutamide and **SK33** treatment resulted in a decreased luciferase activity in all areas. However, mice treated with **SK33** showed a greater reduction of

luciferase activity in these areas when compared to bicalutamide. DMSO vehicle did not significantly affect luciferase activity in any region (Figure 6C).

Tissues were then removed from sacrificed animals, and RNA was extracted and analysed by q-PCR for luciferase transcripts in each individual tissue. Bicalutamide and **SK33** showed strong reduction in luciferase transcripts compared to vehicle or untreated mouse tissues. Although similar, **SK33** reduced luciferase transcripts to a greater extent than bicalutamide – with significantly greater effects in the brain. Neither bicalutamide nor **SK33** had significant effects on AR activity in the spleen. However, **SK33** did not reduce luciferase activity in the leg muscle and showed a significant upregulation of luciferase transcripts in this tissue (Figure 6D). Additionally, both bicalutamide and **SK33** have reduced luciferase enzymatic activity in the prostate, testes and brain. Both anti-androgens showed significant inhibition compared to vehicle control. Although slightly more inhibition was seen in the **SK33** treated mice, the antiandrogens did not show statistically significant differences from each other (Figure 6E).

SK33 is a potent inhibitor of AR in the PTen^{ko} mouse model for prostate intraepithelial neoplasia (PIN).

PTen loss is one of the most frequent events in prostate cancer both at the initiation stage and during late stage metastatic development - found in 30%+ of all human primary prostate cancers, and 60%+ of higher grade metastatic lesions. Wang *et al*, established *Pten*$^{loxp/loxp}$;*Pb-Cre*4 mice, which have conditional *Pten* alleles deleted by a *Probasin* (*Pb*) promoter-driven *Cre* recombinase, limiting *Pten* deletion to the prostatic epithelial layer (32). The mouse model of prostate-specific probasin-mediated *Pten* deletion leads to prostate intraepithelial neoplasia (PIN) leading to adenocarcinoma thereafter. Although the mouse prostate structure is different to human, there are several points of commonality – specifically with the glandular epithelial AR-driven structure.

Pten$^{loxp/loxp}$;*Pb-Cre*4 mice with an integrated androgen reporter were injected sub-cutaneously with 50mg/kg bicalutamide, **SK33** or vehicle (DMSO) control and left for 24hours (n=3 for each treatment). Prostate tissues were collected for qPCR and luciferase assay analysis. Upon q-PCR for luciferase transcripts both anti-androgens showed significant inhibition compared to vehicle control with more inhibition in the **SK33** treated mice than bicalutamide, but the anti-androgens did not show statistically significant difference from

each other (Figure 6F).

In AR^{+ve} mouse $Pten^{ko}$ cells growing in culture (PTEN-CaP8 -ATCC CRL-3033), **SK33** showed a stronger activity than enzalutamide or bicalutamide (Figure 6G).

Discussion

Prostate cancer (PCa), like the prostate gland from which it is derived, is androgen dependent – at least in the initial stages. The inhibition of the androgen receptor activity either by anti-androgen therapy or by androgen ablation remains the mainstay of treatment choices. Recently, there has been a movement away from classical anti-androgens due in part to the development of resistance to these compounds and the advantages of more novel agents e.g. the anti-testosterone synthesis agent abiraterone. Resistance has been historically linked to the development of AR mutations especially in the ligand binding site. For example, AR T887A, W741L and W741C have been found to arise in patients relapsing under flutamide or bicalutamide therapy (7, 8).

However, even in apparent castrate resistant prostate cancer the AR may still be a key molecule to cell growth, and as such remains a viable target for therapeutic intervention. The current clinically used AR antagonists bind the receptor ligand binding site, but with far less efficiency and affinity than natural agonists. The mechanism of the difference between the structure of AR antagonists and partial AR agonists, such as enobosarm, has been associated with the sulfonyl group on the antagonist being larger than the oxygen linker group of the agonist, thus causing a better steric fit. The larger size of the antagonist then pushes away helix 12, inhibiting the folding of the activated AR.

Here we describe the chemical modification of an AR partial agonist – enobosarm. Enobosarm has been shown to have anabolic activity in the body e.g. on bone and muscle mass, but to have minimal effects on the gonadal tissues i.e. an agent with selective AR modulating effects (SARM). The introduction of the 3,5-*Bis*-trifluoromethyl groups was theorized to give bulkier sides to the B ring thus inhibiting helix 12 folding. In essence changing a high affinity agonist to a high affinity antagonist. Two bis-trifluoromethyl-containing enobosarm analogs named **SK33** and **SK51** were the focus of this study.

Initial screening in prostate cancer cell lines indicated that the parental compound, enobosarm, was inactive in all of them, whereas the **SK33** and **SK51**, modified enobosarm analogues showed higher activity (200 fold) in AR^{+ve} cell lines and modest or low activity in AR^{-ve} cell lines. **SK33** showed the highest activity, being more active than the current clinically used anti-androgen – bicalutamide. Treating LNCaP cells with **SK33**, resulted in the inhibition of cell cycle progression, with cells arresting in G1. No apoptotic response or cellular fragmentation was observed. AR inhibition has been associated with the inability of

cells to enter the cell cycle, as the AR may act as a replication licensing protein in prostate cells (33, 34).

The LNCaP cell line is an androgen sensitive cell line with a T877A mutation in the LBD of the AR. Treating this cell line in culture for an extensive period with bicalutamide gave rise to a resistant subclone (LNCaP/BicR) which proliferated in the presence of high doses of bicalutamide, and showed an enhanced expression of AR. This switch to AR agonism is indicative of clinical prostate cancer as it progresses, and this work has been previously reviewed (35, 36). We did not detect other LBD mutations in this cell line. Although not as active as in the parental cell line **SK33** and especially **SK51** showed moderate activity. At this stage it is unclear if the concentration of **SK33** (&**SK51**) required to inhibit the acquired resistance phenotype may be achievable *in vivo*, but their increased metabolic stability, resistance to oxidative metabolism and detoxification together with increased solubility may translate to high levels of drug in circulation. Additionally and of clinical importance, **SK51** showed increased activity over enzalutamide in the LNCaP/BicR cells.

It is rare that an inhibitor compound such as an anti-androgen can be tested in a biological system where there is a highly specific real-time reporter for its target protein activity - integrated into the host genome. Utilizing an LNCaP cell line with an integrated AR-driven luciferase reporter (30) we analyzed the effect of these compounds directly on the transactivation function of the AR. **SK33** resulted in a stronger inhibition of AR-mediated gene activation of both the endogenous gene PSA and the transgene luciferase, than that mediated by bicalutamide. **SK33** could also competitively inhibit the AR in the presence of a strong synthetic androgen (R1881), whilst enobosarm itself had a mildly stimulating effect.

Further testing *in vivo* using unique AR-reporter mice, developed by the authors (31), showed the anti-androgen activity of these compounds in the target tissue i.e. prostate, as well as in peripheral tissues, in real time within the same animal. Here, side effects, and bystander effects could be monitored. **SK33** showed a stronger or equal anti-androgen effect in most tissues, when compared to bicalutamide at the same dosage concentration. But, interestingly we observed that the effects of **SK33** upon leg muscle AR activity was stimulatory, and the effects in the spleen were minimal.

The anabolic effects of enobosarm have been well documented, although its mechanism of action in specifically stimulating skeletal muscle AR and not prostate or gonadal AR remains elusive. Since **SK33** is a modified analog of enobosarm the effects on skeletal muscle was

interesting to observe, especially given its simultaneous high inhibitory activity in the prostate and other tissues. The rational addition of bis-trifluoromethyl groups into ring B of enobosarm seems to have successfully exaggerated the SARM activity of enobosarm. The mechanism of SARM-like compounds remain relatively unknown but locally expressed AR tissue-specific cofactors have been postulated to govern the activity of AR modulating compounds such as SARMs. Although our results are limited to the mouse leg skeletal muscle, the use of such a compound in prostate cancer patients may ease side effects such as muscle wastage and fatigue, whilst maintaining prostate AR inhibition. The effects on other muscle tissues e.g. the AR-responsive levator ani muscle, in the mouse was unavailable.

It should also be noted that **SK33** showed very potent inhibitory effects in the brain - this may reflect the increased lipophilicity of the fluorinated compounds in traversing the blood-brain barrier or in fact their increased anti-androgen potential. The CNS-specific effects could not be determined in the mouse model, but no deleterious effects on motor function or behavior was observed. The effects in humans could well correlate with CNS-related side effects.

Finally, within a developing hyperplasia / adenocarcinoma *in situ* in mice with homozygous PTEN deletion we observed that **SK33** was equal to or better than bicalutamide in reducing AR activity.

Conclusions

We demonstrate that structure-based design can efficiently engineer second-generation AR antagonists that have clinical potential to circumvent anti-androgen resistance by complementing receptor mutations at the molecular level. In principle, there is a limited number of mutations that can cause an AR antagonist to function as an AR agonist, therefore, it is conceivable that such approaches may ultimately lead to the development of anti-androgens that resist mutations that cause anti-androgen withdrawal syndrome.

Utilising novel *in vitro* and *in vivo* screening techniques and models, ideally suited to analyze and evaluate novel antiandrogens, we have identified a novel anti-androgen candidate **SK33.** This bis-trifluoromethyl-containing enobosarm analog**,** displays better activity than bicalutamide *in vitro* with increased efficacy against acquired anti-androgen resistance. Importantly, **SK33** has comparable activity *in vivo*, but maintains a degree of tissue selectivity associated with its SARM – enobosarm parental molecule. The increased stability and potential differential side effect profile of these

molecules may make them useful drugs for prostate cancer treatment.

Materials and Methods

All chemicals were purchased from Sigma Aldrich (Gillingham, United Kingdom) or Alfa Aesar (Heysham, United Kingdom) and were used without further purification. All reactions were performed under a nitrogen atmosphere. H- NMR (500 MHz), C- NMR (125 MHz) and F-NMR (470 MHz) spectra were recorded on a Bruker Avance 500 MHz spectrometer at 25° C. Chemical shifts (δ) are expressed in parts per million (ppm) and coupling constants (J) are given in hertz. The following abbreviations are used in the assignment of NMR signals: s (singlet), bs (broad singlet), d (doublet), t (triplet), q (quartet), m (multiplet), dd (doublet of doublet), dt (doublet of triplet), td (triple doublet), m (multiplet). Mass spectrometry was run on a Bruker Micromass system in electrospray ionization mode. Thin Layer Chromatography (TLC): precoated aluminium backed plates (60 F254, 0.2 mm thickness, Merck) were visualized under both short and long wave UV light (254 and 366 nm). Flash column chromatography was carried out using silica gel supplied by Fisher (60 A°, 35-70 µm). Purity of prepared compounds was determined by Analytical High-Performance Liquid Chromatography (HPLC) analysis using either a ThermoScientific or a Varian Prostar system. All compounds tested in biological assays were > 95% pure. HPLC using the eluents water (eluent A) and acetonitrile (eluent B). Column; Varian Pursuit, 150 mm × 4.6 mm, 5.0 µm. Flow rate; 1.0 mL/min, gradient 30 min 10%

→ 100% eluent B in eluent A.

General method for the preparation of intermediates (3a,b)

Methacryloyl chloride **2** (2.63 mL, 27.16 mmol) was added over the course of 10 minutes to a stirring solution of the different aniline **1a, b** (3.4 mmol) in N,N-dimethylacetamide (10 mL) at r.t. for 3 h. After the reaction was complete, the mixture was diluted with ethyl acetate (100 mL), extracted with sat. aq. $NaHCO_3$ solution (3x25 mL) and with cold brine (4x50 mL). The organic layer was dried over Na_2SO_4 and the solvent was removed at reduced pressure. The crude residue was purified by flash column chromatography.

General method for the preparation of intermediates (4a,b)

To a stirred solution of the intermediates **(3a,b)** (3 mmol) in DCM (7 mL) was added 30% hydrogen peroxide (3.6 mL, 32.03 mmol). The reaction mixture was put in a water bath at r.t. and trifluoroacetic anhydride (3.7 mL, 26.7 mmol) was added slowly to the mixture, which was then stirred for 24 h. The reaction mixture was transferred to a separating funnel using DCM (30 mL). The organic layer was washed with distilled water (20 mL), sat. aq. $Na_2S_2O_3$ (4x20 mL), sat. aq. $NaHCO_3$ (3x20 mL) and brine (20 mL), dried over Na_2SO_4 and concentrated at reduced pressure.

General method for the preparation of compounds SK33 and SK51

To a mixture of NaH (60% in mineral oil, 0.050 g, 1.23 mmol) in anhydrous THF (2 mL) at 0 °C under Ar atmosphere was added a solution of the 3,5-*bis*-trifluoromethylphenol **5** (1.11 mmol) in 1 mL of anhydrous

THF. This mixture was stirred at r.t. for 20 min. A solution of the different intermediates **(4a,b)** (0.74 mmol) in anhydrous THF (3 mL) was added slowly. The reaction mixture was stirred at r.t. o.n. The mixture was then diluted with ethyl acetate (30 mL), washed with brine (15 mL) and water (30 mL), dried over Na_2SO_4 and concentrated under *vacuum*. The crude residue was purified by flash column chromatography.

3-(3,5-bis(trifluoromethyl)phenoxy)-*N*-(4-cyano-3-(trifluoromethyl)phenyl)-2-hydroxy-2-methylpropanamide (SK33)

Purified by flash column chromatography eluting with *n*-hexane/EtOAc 100:0 v/v increasing to *n*-hexane/ EtOAc 90:10 v/v. Obtained in 85 % yield as a white solid.

^{1}H NMR ($CDCl_3$-d_1) δ 9.20 (bs, 1H, NH), 8.16 (d, *J* = 2 Hz, 1H, ArH), 8.00 (dd, *J* = 2, 8.5 Hz, 1H, ArH), 7.82 (d, *J* = 8.5 Hz, 1H, ArH), 7.53 (s, 1H, ArH), 7.36 (s, 2H, ArH), 4.59 (d, *J*= 9 Hz, 1H, CH_2), 4.13 (d, *J* = 9 Hz, 1H, CH2), 3.49 (bs, 1H, OH), 1.67 (s, 3H, CH3); ^{19}F NMR ($CDCl_3$-d_1) δ -62.24, -63.09; ^{13}C NMR ($CDCl_3$-d_1) δ 172.03 (C=O), 158.28 (ArC), 141.29 (ArC) , 135.92 (ArCH), 134.18 (q, $^2J_{C-F}$ = 32.6 Hz, ArC), 133.16 (q, $^2J_{C-F}$ = 33.3 Hz, ArC), 122.94 (q, $^1J_{C-F}$ = 264.5 Hz, CF_3), 122.05 (q, $^1J_{C-F}$ = 272.6 Hz, CF_3), 121.84 (ArCH), 117.33 (q, $^3J_{C-F}$ = 5.1 Hz, ArCH), 115.56 (q, $^3J_{C-F}$ = 3.6 Hz, ArCH), 115.38 (ArC), 115.14 (q, $^3J_{C-F}$ = 3.8 Hz, ArCH), 104.92 (ArC), 75.83 (COH), 73.10 (CH_2), 23.04 (CH_3). MS [ESI, m/z]: 501.1 [M+H], 523.1 [M+Na]. HPLC: retention time = 25.18 min.

3-(3,5-bis(trifluoromethyl)phenoxy)-2-hydroxy-2-methyl-*N*-(4-nitro-2-(trifluoromethyl)phenyl) propanamide (**SK51**)

Purified by flash column chromatography eluting with *n*-hexane/EtOAc 100:0 v/v increasing to *n*-hexane/EtOAc 90:10 v/v. Obtained in 78 % yield as a white solid.

^{1}H NMR ($CDCl_3$-d_1) δ 9.68 (bs, 1H, NH), 8.76 (d, *J* = 9 Hz, 1H, ArH), 8.59 (d, *J* = 3 Hz, 1H, ArH), 8.47 (dd, *J* = 2.5, 9.5 Hz, 1H, ArH), 7.56 (s, 1H, ArH), 7.36 (s, 2H, ArH), 4.59 (d, *J*= 9 Hz, 1H, CH2), 4.15 (d, *J* = 9 Hz, 1H, CH_2), 3.25 (bs, 1H, OH), 1.69 (s, 3H, CH_3); ^{13}F NMR ($CDCl_3$-d_1) δ -61.59, -63.06; ^{13}C NMR ($CDCl_3$-d_1) δ 172.02 (C=O), 158.15 (ArC), 143.17 (ArC), 140.38 (ArC), 133.16 (q, $^2J_{C-F}$ = 33.8 Hz, ArC), 133.03 (q, $^2J_{C-F}$ = 32.8 Hz, ArC), 128.38 (ArCH), 123.22 (q, $^1J_{C-F}$ = 268.3 Hz, CF_3), 122.75 (q, $^1J_{C-F}$ = 271.3 Hz, CF_3),122.62 (ArCH), 122.46 (q, $^3J_{C-F}$ = 6.3 Hz, ArCH), 115.67 (q, $^3J_{C-F}$ = 3.8 Hz, ArCH), 115.11 (ArCH), 75.86 (COH), 73.93 (CH_2), 22.94 (CH_3). MS [ESI, m/z]: 521.1 [M+H], 543.1 [M+Na]. HPLC: retention time = 26.42 min.

Cell culture

All cell lines were purchased LGC Standards (Teddington, UK) and used within 6 passages, and subjected to regular mycoplasma screening (Geneflow PCR test, Lichfield, UK). LNCaP cells were maintained at 37^{o}C, 5% CO_2 in RPMI medium with 10% foetal bovine serum (First Link Ltd, Brierley Hill, U.K.). PC3, VCaP and Du145 and mouse Pten null cells were maintained in DMEM medium (Sigma) with 10% foetal bovine serum (First Link UK,). All media was supplemented with 2mM L-glutamine, 100units/ml penicillin, 100mg/ml streptomycin (Sigma). For hormone depletion experiments, 72 hours before androgen exposure, medium was replaced with 'starvation medium'

consisting of phenol red-free RPMI (or DMEM) medium, supplemented with 5% charcoal-stripped foetal bovine serum (First Link UK). All cell lines were obtained from the ATCC cell bank.

MTT Assay

The MTT assay was used as a cell viability assay for the all the cell lines listed using the anti-androgen compounds. Briefly, cells (5×10^4 cells/ml) were seeded into 96-well plates (200ul/well), allowed to attach and grow for 24hr and subsequently treated with varying concentrations of antiandrogens (0–100 µM) for 96 hours. Optimal seeding densities were premeasured for linear growth over the 96hours. MTT (3-(4,5-dimethylthiazol-2-yl)-2,5-diphenyltetrazolium bromide, 5mg/ml in PBS) was added to a final concentration of 0.5mg/ml for 4 h at 37^{o}C. After four hours, purple formazan crystals, formed by mitochondrial reduction of MTT, were solubilized in acidified isopropanol (200µl/ well) and the absorbance was read at 570 nm after 10 min incubation. Percent inhibition of viability was calculated as a % of untreated control and the cytotoxicity / cell growth inhibition was expressed as IC_{50}**.**

Luciferase Assays

Cells were washed and lysed in reporter lysis buffer (Promega). Lysate was mixed with *D*-luciferin substrate (Promega) and light emission measured using the Promega Glomax multi luminometer.
For live cell imaging *D*-luciferin substrate was added directly into the cell media and plates were imaged on a Syngene G:Box imager.
Tissue was pulverized by grinding in liquid nitrogen and then completely homogenised, using a microfuge pestle, in reporter lysis buffer with protease inhibitors (Promega). Lysate (20µl) was mixed with luciferin substrate (20µl) and light emission measured using the Promega Glomax multi luminometer. Light emission was then normalised to protein content as measured by a Bradford Assay.

RNA extraction and RT-PCR

Total RNA samples were prepared using Trizol reagent (Sigma) and converted to cDNA using the GoScript™ Reverse Transcription System (Promega).

Q-PCR

Reactions were performed in triplicate on cDNA samples in 96-well optical plates on an ABI Prism StepOne System (ThermoFisher, U.K.). Reactions consisted of 2 µl cDNA, 7 µl PCR-grade water, 10 µl 2× TaqMan Universal PCR Master Mix (Applied Biosystems), 1 µl Taqman specific assay probes

(Applied Biosystems) for PSA, TMPRSS2, KLK2, and L19. Parameters were: 50°C for 2 min, 95°C for 10 min, 40 cycles of 95°C for 15 sec and 60°C for 1 min. Data was recorded using Sequence Detector Software (SDS version 2.3; PE Applied Biosystems). Levels were normalised to GAPDH, β-actin and RPL19.

Animal experiments

All mouse procedures were performed in accordance with the UK Animals (Scientific Procedures) Act 1986 under Home Office license. ARE-Luc strains were made and available 'in house' (31), and *Pten*$^{loxp/loxp}$;*Pb-Cre4* were obtained from The Jackson Laboratory.

Luciferase imaging

Anaesthetized mice (3% isofluorane with O_2 carrier, Abbott Animal Health UK) were injected *i.p.* or *s.c.* with *D*-luciferin (Caliper Life Sciences Ltd, Runcorn, UK) at 150 mg/kg, 10 min before imaging. Light emission from luciferase was detected by the IVIS Imaging System 100 series (Xenogen Corporation), and overlaid as a pseudocolour image with reference scale, upon a greyscale optical image.

For *ex vivo* imaging, mice were sacrificed 10 min after luciferin injection, and immediately dissected. Target organs were rinsed briefly in PBS and placed under the bioluminescent camera. Tissues were then collected for luciferase assays, RNA extraction or fixed in 10% formaldehyde before wax embedding and sectioned using standard procedures.

Cell cycle analysis (FACS)

Cells were grown on 10cm dishes for 24-96 h ± treatments. Cells were then trypsinized, washed twice in PBS, fixed in 70% ethanol at 4 °C, were stained with 5 μg/ml propidium iodide and RNA removed using 50 mg/ml RNase A. FACSanalysis was carried out using a FACSCalibur (Beckton-Dickinson, Oxford, UK), using linear scale representation of forward and side scatter during flow analysis, as well as DNA content. Single cells were gated and the cell cycle profiles measured using FCS Express4 software, using the built in kinetics & cell cycle analysis best-fit model for cell cycle phase identification. A total of 10 000 events were measured per sample.

Acknowledgments

The authors would like to pay a tribute to Professor Christopher McGuigan (the Drug Hunter) for all his contributions for the success of this project. Professor McGuigan was an exceptional and

dedicated scientist who has remarkable achievements in the anticancer and antiviral drug discovery field.

The authors would like to thank Cyprotex (U.K.) for performing the metabolic stability, PPB % recovery, hERG inhibition assays as an outsourced service. We would also like to thank our funders - The Welsh Government (A4B-Academic Expertise for Business grant), The Cardiff University – Peking University Cancer Institute, Prostate Cancer UK, Cancer Research UK and the Harvey Spack memorial Fellowship (GSA).

References

1. Ferlay J, Autier P, Boniol M, Heanue M, Colombet M, Boyle P. Estimates of the cancer incidence and mortality in Europe in 2006. Ann Oncol. 2007;18(3):581-92.
2. Brinkmann AO, Trapman J. Prostate cancer schemes for androgen escape. Nat Med. 2000;6(6):628-9.
3. Brinkmann AO. Molecular mechanisms of androgen action--a historical perspective. Methods Mol Biol. 2011;776:3-24.
4. Matsumoto T, Shiina H, Kawano H, Sato T, Kato S. Androgen receptor functions in male and female physiology. J Steroid Biochem Mol Biol. 2008;109(3-5):236-41.
5. Patrão MT, Silva EJ, Avellar MC. Androgens and the male reproductive tract: an overview of classical roles and current perspectives. Arq Bras Endocrinol Metabol. 2009;53(8):934-45.
6. Manolagas SC, Kousteni S, Jilka RL. Sex steroids and bone. Recent Prog Horm Res. 2002;57:385-409.
7. Hara T, Miyazaki J, Araki H, Yamaoka M, Kanzaki N, Kusaka M, et al. Novel mutations of androgen receptor: a possible mechanism of bicalutamide withdrawal syndrome. Cancer Res. 2003;63(1):149-53.
8. Suzuki H, Akakura K, Komiya A, Aida S, Akimoto S, Shimazaki J. Codon 877 mutation in the androgen receptor gene in advanced prostate cancer: relation to antiandrogen withdrawal syndrome. Prostate. 1996;29(3):153-8.
9. Brooke GN, Bevan CL. The role of androgen receptor mutations in prostate cancer progression. Curr Genomics. 2009;10(1):18-25.
10. Paliouras M, Zaman N, Lumbroso R, Kapogeorgakis L, Beitel LK, Wang E, et al. Dynamic rewiring of the androgen receptor protein interaction network correlates with prostate cancer clinical outcomes. Integr Biol (Camb). 2011;3(10):1020-32.
11. McEwan IJ. Androgen receptor modulators: a marriage of chemistry and biology. Future Med Chem. 2013;5(10):1109-20.
12. Jones A, Coss CC, Steiner MS, Dalton JT. An Overview on Selective Androgen Receptor Modulators. Focus on Enobosarm.: Drugs of the Future; 2013. p. 309-16.
13. Dalton JT, Barnette KG, Bohl CE, Hancock ML, Rodriguez D, Dodson ST, et al. The selective androgen receptor modulator GTx-024 (enobosarm) improves lean body mass and physical function in healthy elderly men and postmenopausal women: results of a double-blind, placebo-controlled phase II trial. J Cachexia Sarcopenia Muscle. 2011;2(3):153-61.
14. Dalton JT, Taylor RP, Mohler ML, Steiner MS. Selective androgen receptor modulators for the prevention and treatment of muscle wasting associated with cancer. Curr Opin Support Palliat Care. 2013;7(4):345-51.
15. Kim J, Wu D, Hwang DJ, Miller DD, Dalton JT. The para substituent of S-3-(phenoxy)-2-hydroxy-2-methyl-N-(4-nitro-3-trifluoromethyl-phenyl)-propionamides is a major structural determinant of in vivo disposition and activity of selective androgen receptor modulators. J Pharmacol Exp Ther. 2005;315(1):230-9.
16. Hashimoto Y, Miyachi H. Nuclear receptor antagonists designed based on the helix-folding inhibition hypothesis. Bioorg Med Chem. 2005;13(17):5080-93.
17. Duke CB, Jones A, Bohl CE, Dalton JT, Miller DD. Unexpected binding orientation of bulky-B-ring anti-androgens and implications for future drug targets. J Med Chem. 2011;54(11):3973-6.

18. Weatherman RV, Fletterick RJ, Scanlan TS. Nuclear-receptor ligands and ligand-binding domains. Annu Rev Biochem. 1999;68:559-81.
19. McGinley PL, Koh JT. Circumventing anti-androgen resistance by molecular design. J Am Chem Soc. 2007;129(13):3822-3.
20. Ferla S, Bassetto M, Pertusati F, Kandil S, Westwell AD, Brancale A, et al. Rational design and synthesis of novel anti-prostate cancer agents bearing a 3,5-bis-trifluoromethylphenyl moiety. Bioorg Med Chem Lett. 2016;26(15):3636-40.
21. Purser S, Moore PR, Swallow S, Gouverneur V. Fluorine in medicinal chemistry. Chem Soc Rev. 2008;37(2):320-30.
22. Hagmann WK. The many roles for fluorine in medicinal chemistry. J Med Chem. 2008;51(15):4359-69.
23. Swallow S. Fluorine in medicinal chemistry. Prog Med Chem. 2015;54:65-133.
24. Xing L, Blakemore DC, Narayanan A, Unwalla R, Lovering F, Denny RA, et al. Fluorine in drug design: a case study with fluoroanisoles. ChemMedChem. 2015;10(4):715-26.
25. Prchalová E, Štěpánek O, Smrček S, Kotora M. Medicinal applications of perfluoroalkylated chain-containing compounds. Future Med Chem. 2014;6(10):1201-29.
26. Kandil S, Westwell AD, McGuigan C. 7-Substituted umbelliferone derivatives as androgen receptor antagonists for the potential treatment of prostate and breast cancer. Bioorg Med Chem Lett. 2016;26(8):2000-4.
27. Kandil S, Wymant JM, Kariuki BM, Jones AT, McGuigan C, Westwell AD. Novel cis-selective and non-epimerisable C3 hydroxy azapodophyllotoxins targeting microtubules in cancer cells. Eur J Med Chem. 2016;110:311-25.
28. Horoszewicz JS, Leong SS, Kawinski E, Karr JP, Rosenthal H, Chu TM, et al. LNCaP model of human prostatic carcinoma. Cancer Res. 1983;43(4):1809-18.
29. Korenchuk S, Lehr JE, MClean L, Lee YG, Whitney S, Vessella R, et al. VCaP, a cell-based model system of human prostate cancer. In Vivo. 2001;15(2):163-8.
30. Dart DA, Spencer-Dene B, Gamble SC, Waxman J, Bevan CL. Manipulating prohibitin levels provides evidence for an in vivo role in androgen regulation of prostate tumours. Endocr Relat Cancer. 2009;16(4):1157-69.
31. Dart DA, Waxman J, Aboagye EO, Bevan CL. Visualising androgen receptor activity in male and female mice. PLoS One. 2013;8(8):e71694.
32. Wang S, Gao J, Lei Q, Rozengurt N, Pritchard C, Jiao J, et al. Prostate-specific deletion of the murine Pten tumor suppressor gene leads to metastatic prostate cancer. Cancer Cell. 2003;4(3):209-21.
33. D'Antonio JM, Vander Griend DJ, Isaacs JT. DNA licensing as a novel androgen receptor mediated therapeutic target for prostate cancer. Endocr Relat Cancer. 2009;16(2):325-32.
34. Koushyar S, Economides G, Zaat S, Jiang W, Bevan CL, Dart DA. The prohibitin-repressive interaction with E2F1 is rapidly inhibited by androgen signalling in prostate cancer cells. Oncogenesis. 2017;6(5):e333.
35. Paul R, Breul J. Antiandrogen withdrawal syndrome associated with prostate cancer therapies: incidence and clinical significance. Drug Saf. 2000;23(5):381-90.
36. Visakorpi T, Hyytinen E, Koivisto P, Tanner M, Keinänen R, Palmberg C, et al. In vivo amplification of the androgen receptor gene and progression of human prostate cancer. Nat Genet. 1995;9(4):401-6.

Tables:

	Metabolic stability (t1/2 mins)	Plasma protein binding assay (PPB) %	%hERG inhibition at 25µM
Bicalutamide	214	n.d.	96 *
SK33	1930	94.7	7.64

Table 1. t1/2 calculated in human liver microsomes; SK33 is metabolically stable with no loss of parent compound detected for the duration of the assay. Plasma protein binding (PPB) assay; results are expressed in terms of mean % bound from duplicate experiments. Cardiotoxicity expressed in terms of % hERG inhibition at 25 µM compound concentration.

Figure legends

Figure 1.

A, Chemical structure of the clinically used non-steroidal antiandrogens; flutamide, hydroxylflutamide, nilutamide, bicalutamide and enzalutamide showing rings A and B. **B**, Chemical structure of enobosarm (left), SK33 and SK51 (right). **C**, Chemical synthesis of SK33 and SK51 compounds, reagents and conditions: i) DMA, rt, 24h, ii) H2O2, DCM, rt, 2h, iii) NaH, THF, rt, 24 h.

Figure 2.

(A, B) X-ray structure of enobosarm (red-carbons) co-crystallised with (AR wt) in the agonist conformation showing the orientation the distal ring B extending away from Helix 12 (H12) towards Trp741. (**C, D**) Overlaid predicted binding modes of SK33-R (pink carbons), SK33-S (turquoise carbons) and enobosarm (grey carbons) inside the AR-LBD showing the orientation of ring B with the bis-CF3 groups inducing geometric bulk keeping Helix 12 in the antagonist conformation (open) even upon the development of adaptive (resistant) bulk reducing mutations.

Figure 3. Enobosarm analogues SK33 and SK51 show potent and selective activity in AR positive prostate cancer cells.

MTT cytotoxicity assays of LNCaP cells treated with increasing doses of enobosarm or SK33 (**A**) or Bicalutamide, SK33 and SK51 (**B**) at 0-100μM. MTT cytotoxicity assays of PC3 cells treated with increasing doses of enobosarm or SK33 (**C**) or Bicalutamide, SK33 and SK51 (**D**) at 0-100μM for 96hr. **E**, Q-PCR analysis of a panel of prostate cancer cells for AR expression. Data represents the mean of three independent experiments. Data was normalised to GAPDH, β-actin and RPL19 housekeeping genes. **F**, Bar chart representing a summary of the IC_{50} values for the 4 cell lines listed according to their AR status. **G**, FACS analysis of LNCaP cells treated with 10μM bicalutamide, enzalutamide, SK33, SK51 or vehicle control for 48hours, and analysed for S phase (left hand side). Histograms showing DNA content (PI fluorescence) of treated LNCaP cells (right hand side). **H**, FACS analysis of PC3 cells treated with 10μM bicalutamide, enzalutamide, SK33, SK51 or vehicle control for 48hours, and

analysed for S phase (left hand side). Histograms showing DNA content (PI fluorescence) of treated PC3 cells (right hand side). 10,000 gated cells were measured for each experiment.

Figure 4. SK33 and SK51 inhibit AR-mediated transcriptional activity in prostate cancer cells.

A, Schematic diagram of the activation of the synthetic androgen reporter construct integrated into the LNCaP/ARE-Luc cell line. Ligand bound AR activates the expression of the luciferase reporter gene which in the presence of luciferin substrate gives off bioluminescence directly proportional to AR activity. **B**, Q-PCR analysis of the endogenous androgen induced gene PSA and the transgenes luciferase and G418 (Neomycin resistance gene - aminoglycoside 3'-phosphotransferase) in LNCaP/ARE-Luc cells. Cells were grown for 72hours in charcoal stripped FCS and then treated with 0-10 nM R1881. Data represents the mean of three independent experiments. Data was normalised to GAPDH, β-actin and RPL19 housekeeping genes. **C**, Q-PCR analysis of PSA gene expression in LNCaP cells grown in charcoal stripped medium for 72hours and then treated with R1881 in the presence of increasing concentrations of bicalutamide or SK33 (0-10 μM) or enobosarm (**D**). Data represents the mean of three independent experiments. Data was normalised to GAPDH, β-actin and RPL19 housekeeping genes. **E**, Grey scale image of bioluminescence from live LNCaP/Luc cells treated with enobosarm, SK33 and bicalutamide (0-100 μM) for 24 hours. **F**, Line graph indicating bioluminescence activity measurements from LNCaP/Luc cells treated with increasing concentrations of bicalutamide, enobosarm and SK33 for 24 hours. ** = p>0.01.

Figure 5. SK33 is active in LNCaP cells with acquired bicalutamide resistance.

A, Bar graph indicating the relative expression levels of AR in LNCaP and LNCaP/BicR cells. Data represents the mean of three independent experiments. Data was normalised to GAPDH, β-actin and RPL19 housekeeping genes. **B&C**, MTT cytotoxicity assays of LNCaP or LNCaP/BicR cells treated with increasing concentrations of bicalutamide (**B**) or enzalutamide

(**C**) for 96 hours. **D**, MTT cytotoxicity assays of LNCaP/Bic20 cells treated with increasing concentrations of bicalutamide, SK33 and SK51 for 96 hours.

Figure 6. SK33 inhibits AR transcriptional activity in vivo and in prostate intraepithelial neoplasia (PIN).

A, Bioluminescent imaging of live ARE-Luc mice pre and post treatment with bicalutamide or SK33 (or DMSO vehicle) for 24 hours. Image represents a grey scale image overlaid with pseudo-colour bioluminescent activity data (scale represents flux rate of photons/sec/cm2). **B**, grey scale image of an ARE-Luc mouse, white circles represent the three regions of interest measurements for each mouse. **C**, Bar graph representing relative bioluminescent data emanating from the three regions of interest - head, abdomen and gonadal regions. Data is normalised to mouse bioluminescence pre-treatment with bicalutamide, SK33 (50 mg/kg) or DMSO vehicle. **D**, Q-PCR analysis of luciferase expression from various body tissues as indicated. Data is presented as luciferase / housekeeping genes (GAPDH, RPL19 and β-actin). **E**, Bar graph indicating relative luciferase enzymatic activity from various tissues from ARE-Luc mice treated with either bicalutamide, SK33 or DMSO. **F**, Q-PCR analysis of luciferase expression from the mouse $PTen^{ko}$ prostate tissues. Data is presented as luciferase / housekeeping genes (GAPDH, RPL19 and β-actin). **G**, MTT assay of PTen null mouse prostate cells treated with increasing doses of bicalutamide, enzalutamide and SK33 for 96hours. *= p value 0.05, ** = p value 0.01.

Figure 1.

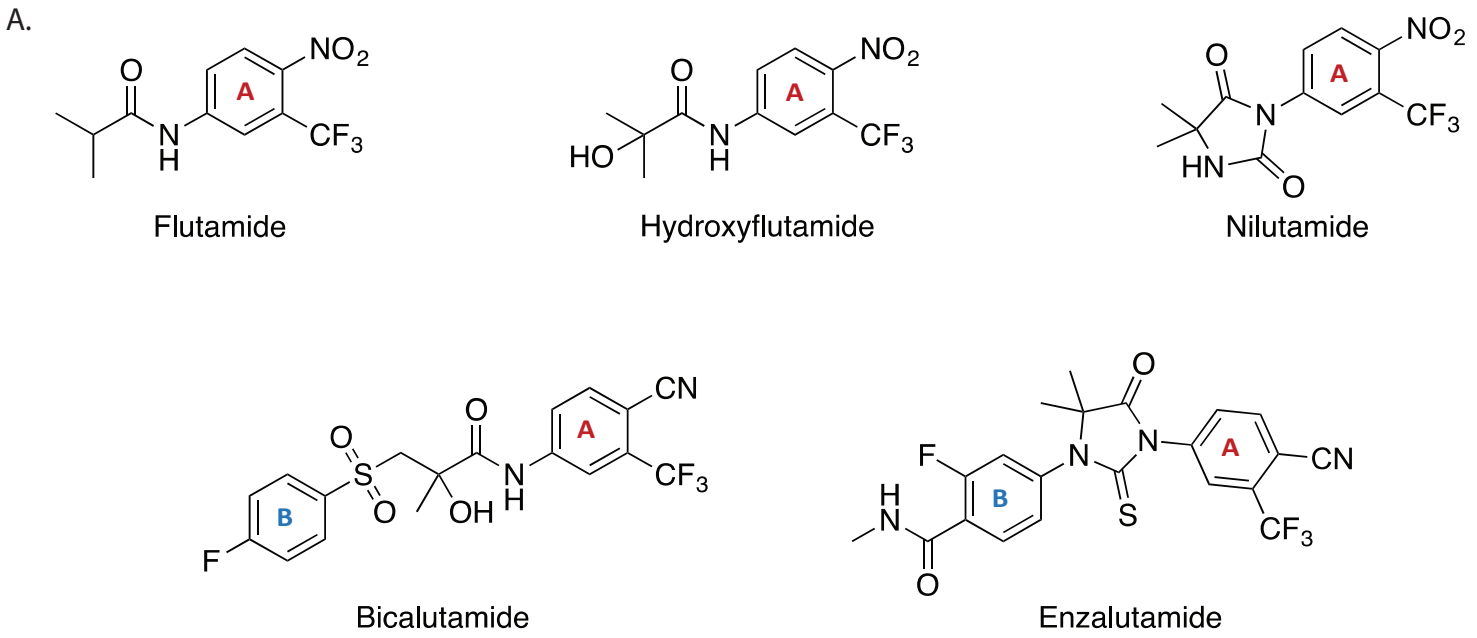
A.
Flutamide
Hydroxyflutamide
Nilutamide
Bicalutamide
Enzalutamide

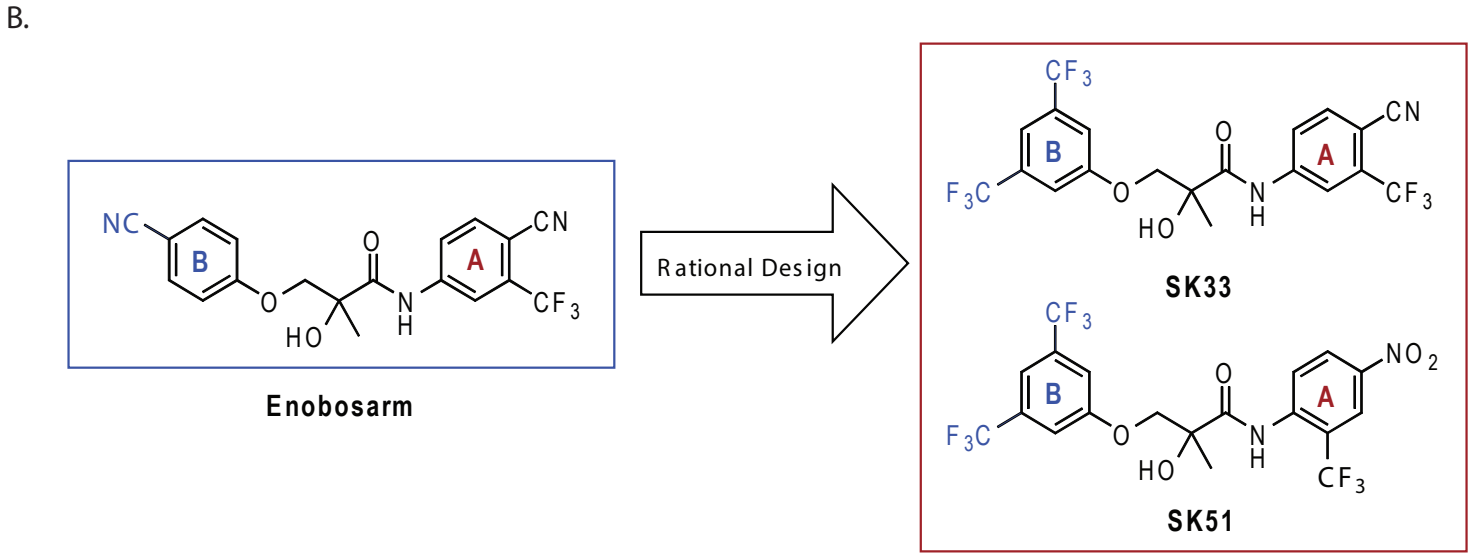
B.
Enobosarm
Rational Design
SK33
SK51

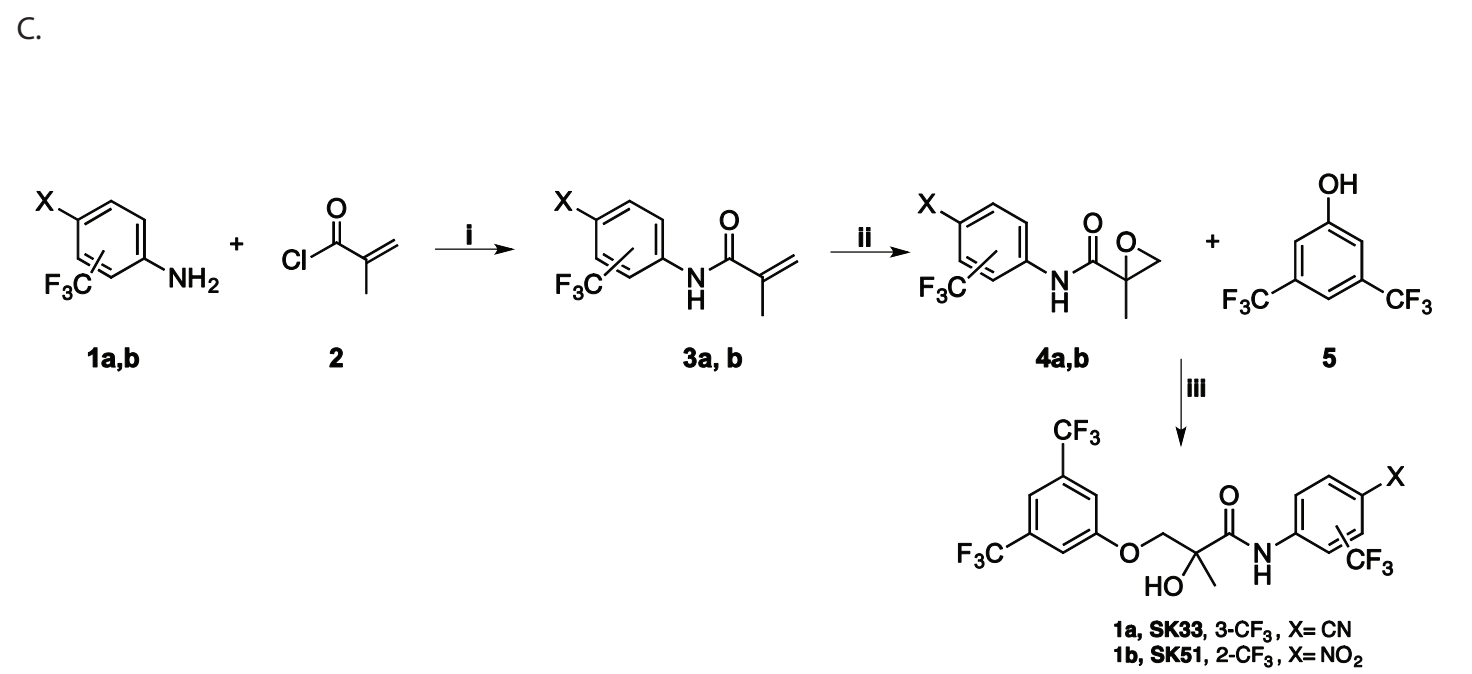
C.
1a,b
2
3a, b
4a,b
5
i
ii
iii
1a, SK33, 3-CF3, X= CN
1b, SK51, 2-CF3, X= NO2

Figure 2.

A.

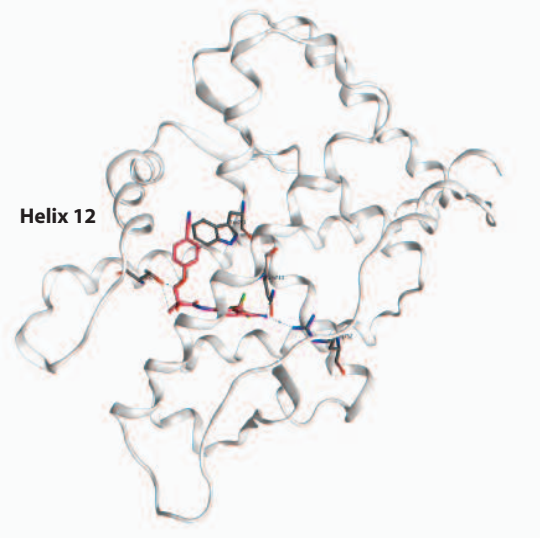

B.

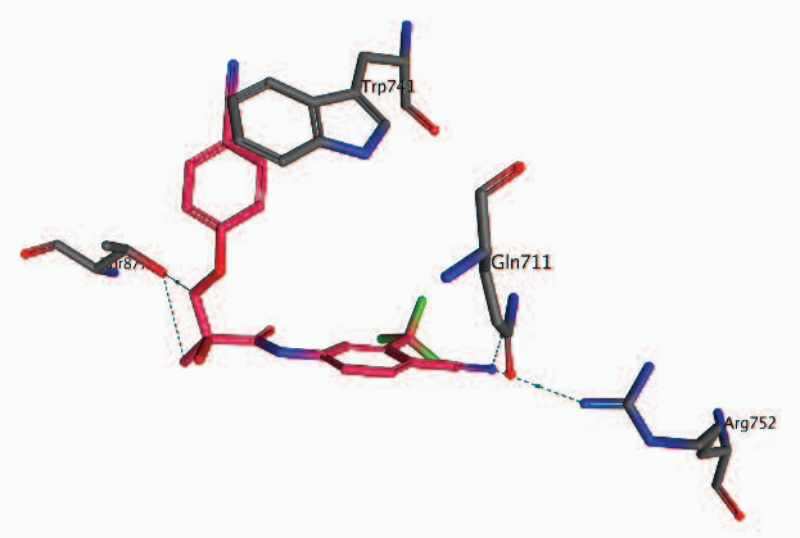

C.

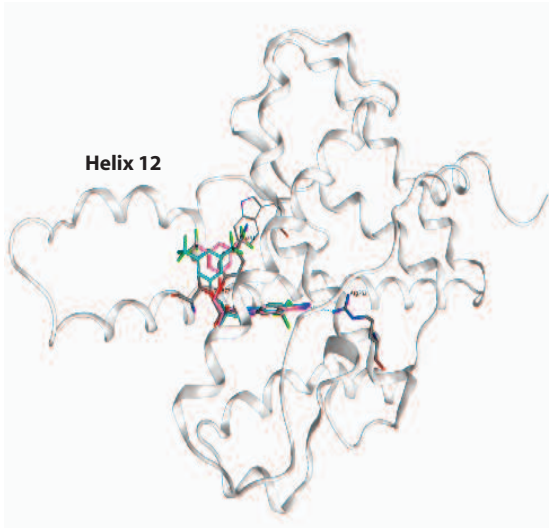

D.

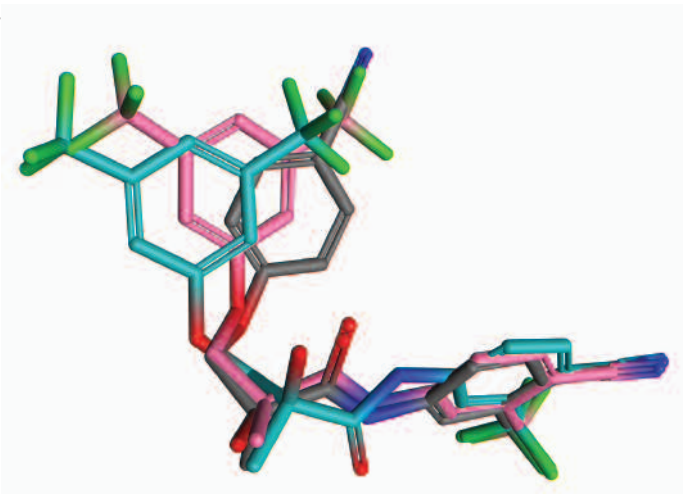

Figure 3.

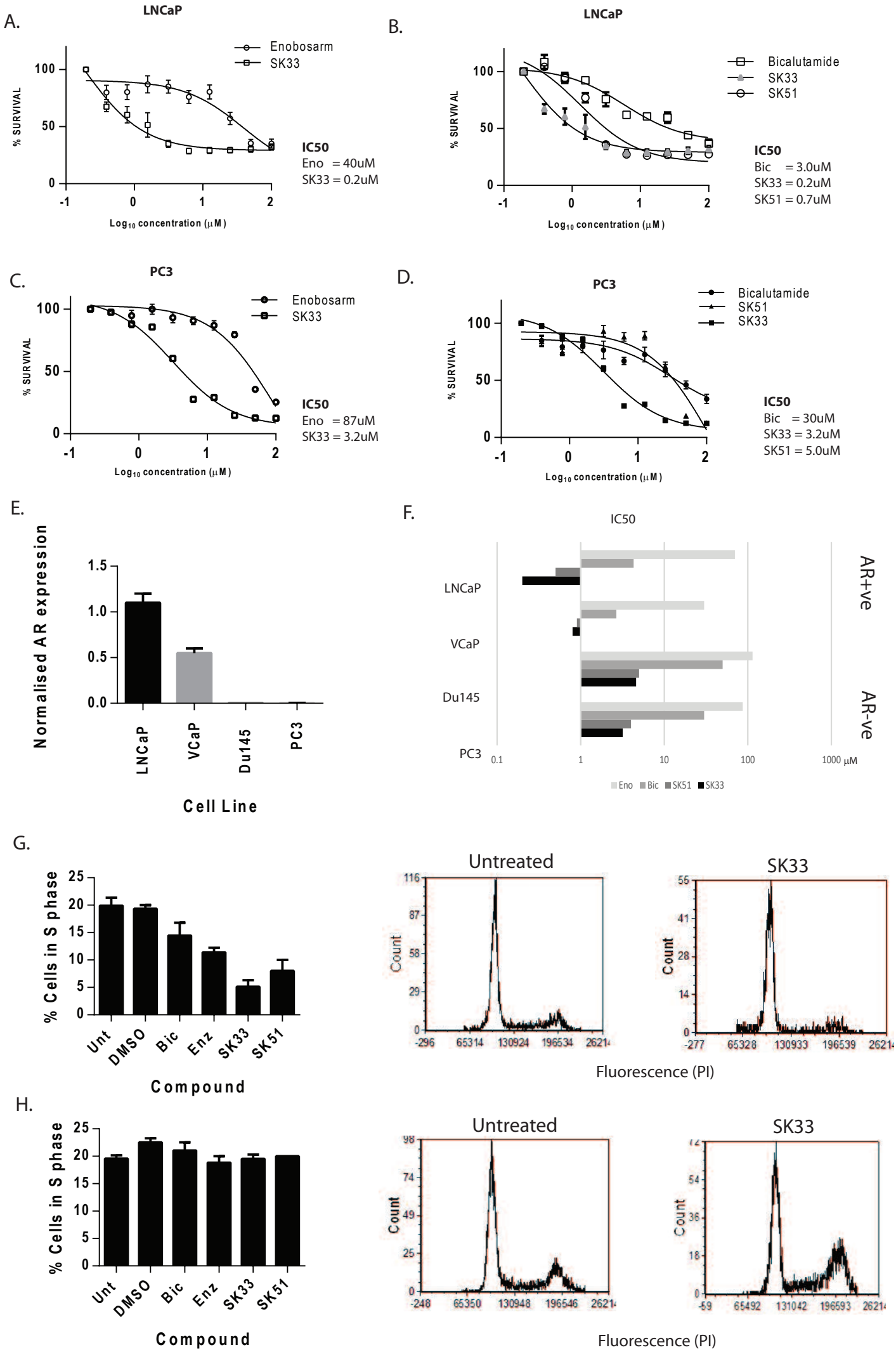
A.
LNCaP
Enobosarm
SK33
% SURVIVAL
Log10 concentration (μM)
IC50
Eno = 40uM
SK33 = 0.2uM
B.
LNCaP
Bicalutamide
SK33
SK51
% SURVIVAL
Log10 concentration (μM)
IC50
Bic = 3.0uM
SK33 = 0.2uM
SK51 = 0.7uM
C.
PC3
Enobosarm
SK33
% SURVIVAL
Log10 concentration (μM)
IC50
Eno = 87uM
SK33 = 3.2uM
D.
PC3
Bicalutamide
SK51
SK33
% SURVIVAL
Log10 concentration (μM)
IC50
Bic = 30uM
SK33 = 3.2uM
SK51 = 5.0uM
E.
Normalised AR expression
LNCaP
VCaP
Du145
PC3
Cell Line
F.
IC50
LNCaP
VCaP
Du145
PC3
AR+ve
AR-ve
Eno
Bic
SK51
SK33
G.
% Cells in S phase
Unt
DMSO
Bic
Enz
SK33
SK51
Compound
Untreated
SK33
Count
Fluorescence (PI)
H.
% Cells in S phase
Unt
DMSO
Bic
Enz
SK33
SK51
Compound
Untreated
SK33
Count
Fluorescence (PI)

Figure 4.

A.

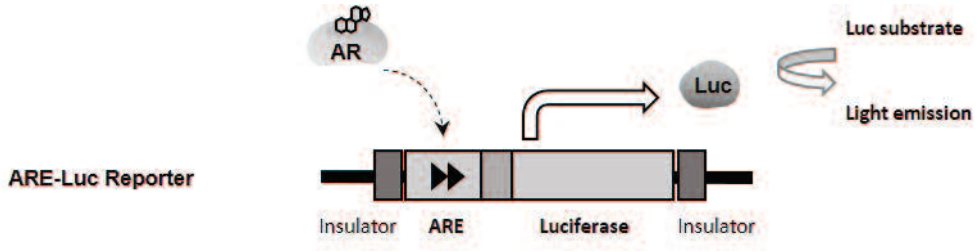

B.

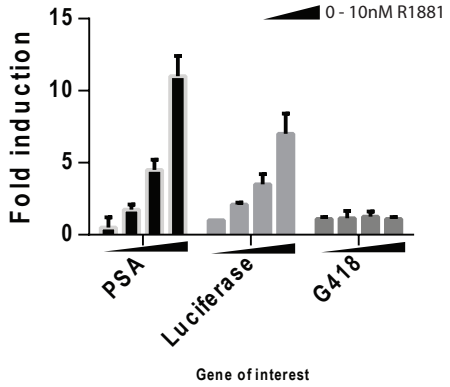

C.

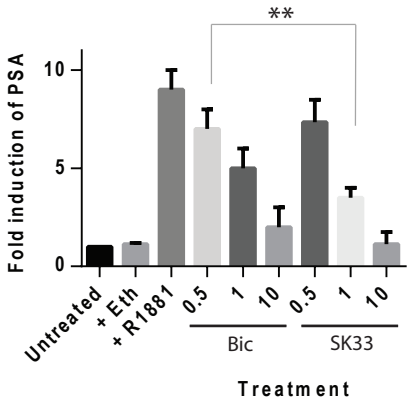

D.

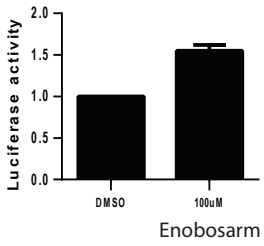

E.

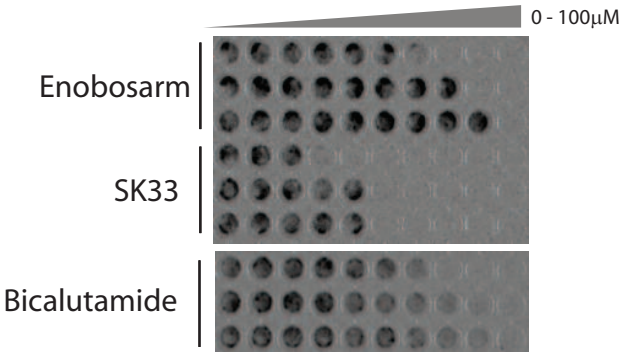

F.

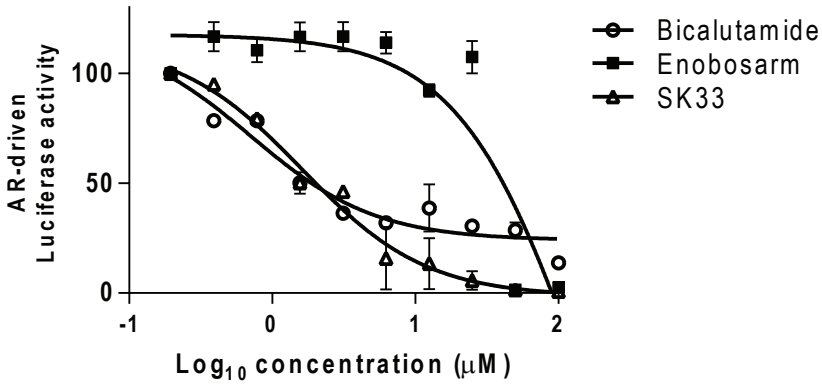

Figure 5.

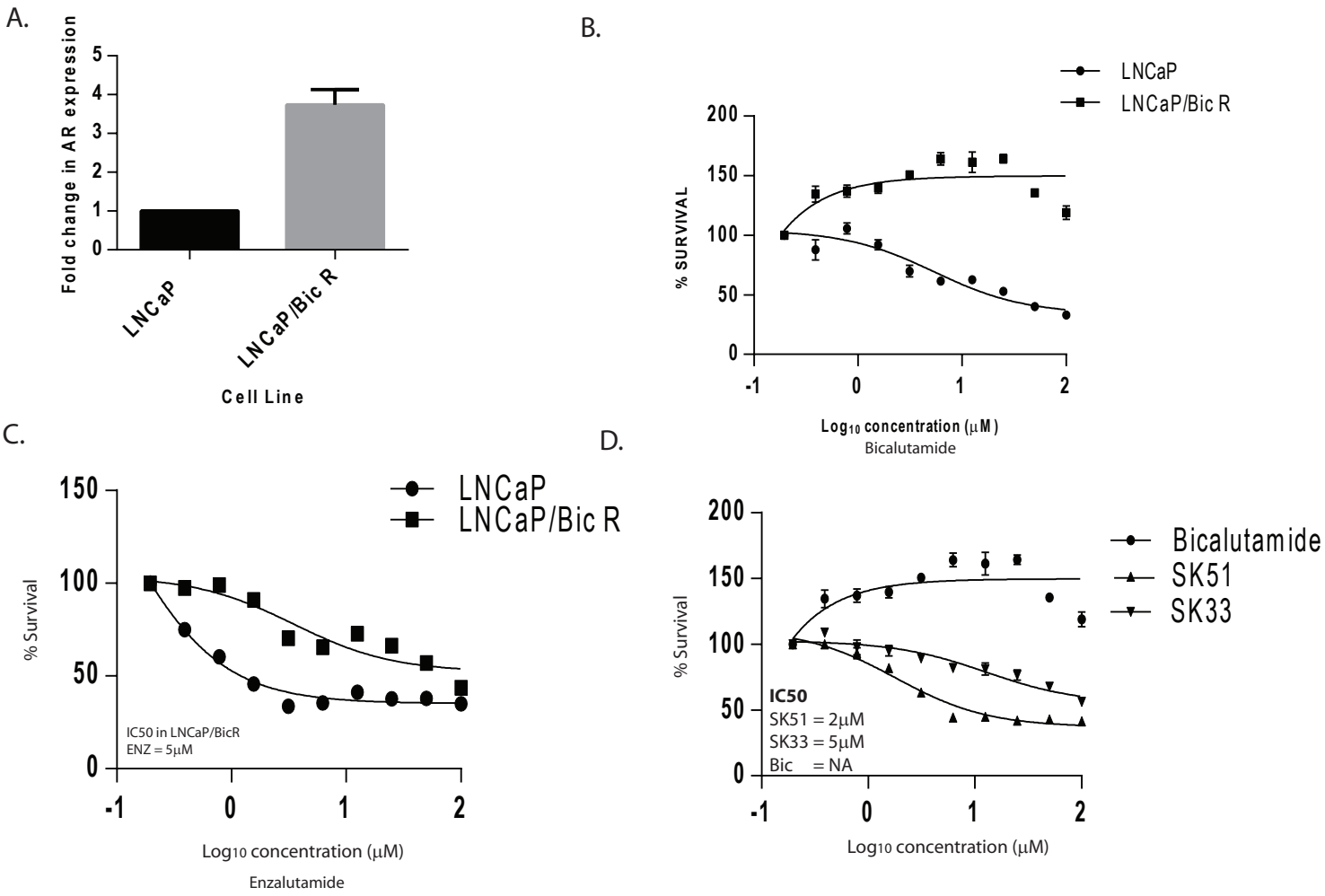
A.
Fold change in AR expression
0
1
2
3
4
5
LNCaP
LNCaP/Bic R
Cell Line
B.
LNCaP
LNCaP/Bic R
% SURVIVAL
0
50
100
150
200
-1
0
1
2
Log10 concentration (μM)
Bicalutamide
C.
LNCaP
LNCaP/Bic R
% Survival
0
50
100
150
IC50 in LNCaP/BicR
ENZ = 5μM
-1
0
1
2
Log10 concentration (μM)
Enzalutamide
D.
Bicalutamide
SK51
SK33
% Survival
0
50
100
150
200
IC50
SK51 = 2μM
SK33 = 5μM
Bic = NA
-1
0
1
2
Log10 concentration (μM)

Figure 6.

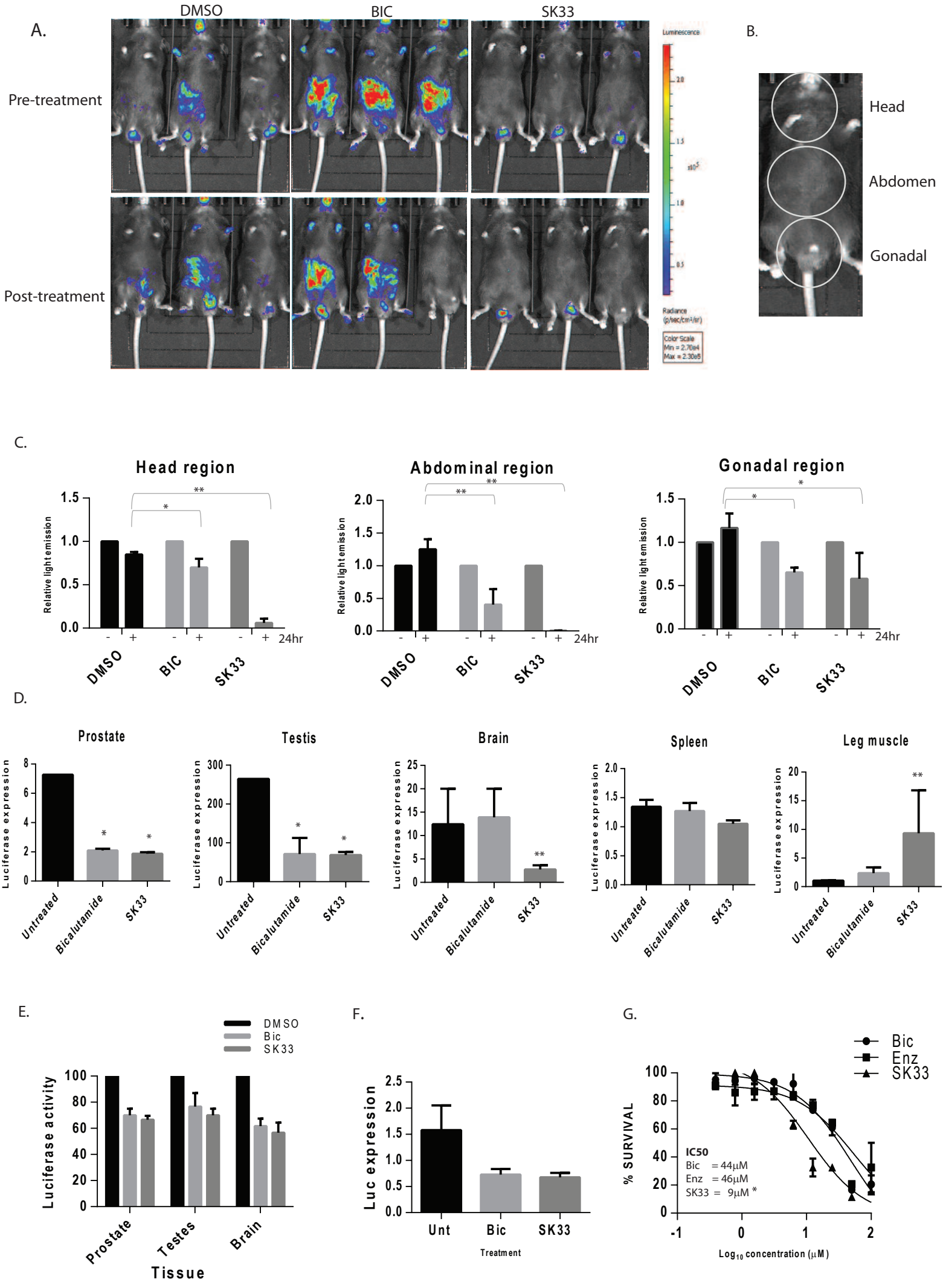
A.
DMSO
BIC
SK33
Pre-treatment
Post-treatment
Luminescence
Radiance (p/sec/cm²/sr)
Color Scale
Min = 2.70e4
Max = 2.30e5
B.
Head
Abdomen
Gonadal
C.
Head region
Abdominal region
Gonadal region
Relative light emission
24hr
DMSO
BIC
SK33
D.
Prostate
Testis
Brain
Spleen
Leg muscle
Luciferase expression
Untreated
Bicalutamide
SK33
E.
DMSO
Bic
SK33
Luciferase activity
Prostate
Testes
Brain
Tissue
F.
Luc expression
Unt
Bic
SK33
Treatment
G.
Bic
Enz
SK33
% SURVIVAL
IC50
Bic = 44μM
Enz = 46μM
SK33 = 9μM *
Log10 concentration (μM)